CHANGES IN SOLAR IRRADIANCE AND ATMOSPHERIC TURBIDITY IN COSTA RICA DURING THE TOTAL SOLAR ECLIPSE OF JULY 11, 1991

WALTER FERNÁNDEZ AND VILMA CASTRO

Laboratory for Atmospheric and Planetary Research, School of Physics and Center for Geophysical Research, University of Costa Rica, San José, Costa Rica

JAIME WRIGHT

Department of Physics, National University, Heredia, Costa Rica

HUGO HIDALGO

National Meteorological Institute, Ministry of Natural Resources, Energy, and Mines, San José, Costa Rica

ALEJANDRO SÁENZ

School of Physics, and Material Science and Engineering Research Center, University of Costa Rica, San José, Costa Rica

Abstract. Solar global radiation was measured in several places in Costa Rica during the total solar eclipse that occurred on July 11, 1991. In two of these places, Puntarenas and Santa Cruz, measurements in the ultraviolet range (295–385 nm) were also taken. In Santa Cruz, a normal incidence pyrheliometer with Schott filters OG530 and RG630 was used to measure direct solar radiation in its whole range, and in the 530–2800 nm and 630–2800 wavebands respectively. Global radiation, and consequently direct, diffuse and irradiance in any of the wavebands considered, decreased gradually as the sun was being eclipsed and reached zero during the totality, then increased to their normal values. Data registered in Santa Cruz were used to determine Ångstrom's atmospheric turbidity parameters α and β. Computations show that between 13:00 and 14:30 LT (local time), α decreased and β increased significantly. This indicates that atmospheric turbidity was high and large particles were more abundant than small ones. The size of hygroscopic particles increased during the eclipse when temperature decreased and relative humidity increased in a comparatively short time.

1. Introduction

On July 11, 1991 a total solar eclipse took place. It started over the Pacific Ocean near Hawaii, crossed the ocean, and advanced southeast through the coast of Mexico, Central America, Colombia and Brazil.

The general characteristics of the eclipse are described in Fernández *et al.* (1992). Over Costa Rica, along the central line of the umbra, the totality had an average duration of five and a half minutes. In Peñas Blancas (northern border) the first contact occurred by 12:40 LT (local time) and the beginning of totality by 14:01 LT. In Paso Canoas (southern border) the first contact occurred by 12:50

Earth, Moon, and Planets **63**: 119–132, 1993.

LT (about ten minutes later than in Peñas Blancas) and the beginning of totality near 14:09 LT. Last contact was near 15:17 LT in Peñas Blancas and 15:23 LT in Paso Canoas. Similar information for other localities can be found in a number of publications (e.g. Fernández *et al.*, 1992).

Measurements of solar irradiance and other atmospheric parameters were taken in several places in Costa Rica. In this article, changes in solar irradiance, and Ångstrom's atmospheric turbidity parameters α and β, during the eclipse, are presented. Changes in air temperature and wind speed are described in Fernández *et al.* (1993, this issue).

2. Instruments and Observation Sites

Some meteorological stations in Costa Rica are equipped with bimetallic actinographs. These instruments have a slow response and are inappropriate for measuring instantaneous values of irradiance. For this reason, fast response photoelectric cells were installed in Santa Cruz, Puntarenas, Damas, Tárcoles, and Filadelfia (Figure 1). Solar global radiation was measured with black and white Eppley model 8–48 pyranometers, with glass domes uniformly transparent from 285 to 2800 nm.

In Santa Cruz and Puntarenas, Eppley ultraviolet (UV) pyranometers (295 to 385 nm) were also installed, and in Santa Cruz an Eppley normal incidence pyrheliometer (NIP) with a solar tracker was installed. This was used to measure direct incident radiation in several wavebands, with filters OG530 (transparent from 530 to 2800 nm) and RG630 (transparent from 630 to 2800 nm).

3. Global Radiation

Figures 2 and 3 show the changes in solar global radiation intensity over the observation sites. In all sites intensity decreased progressively as the sun was being eclipsed, and became negligible during the totality. As an example, in Puntarenas, it decreased from around 1000 Wm^{-2} at 12:40 LT to 0 Wm^{-2}.

4. Direct and Diffuse Radiation

For any zenith angle θ, *global radiation* I_g is given by (Paltridge and Platt, 1971):

$$I_g = I_n \cos\theta + \int i_d \, \mathrm{d}\Omega \,, \tag{1}$$

where I_n is normal incidence irradiance and i_d is diffuse irradiance, whose contribution must be integrated over all solid angles of the sky hemisphere.

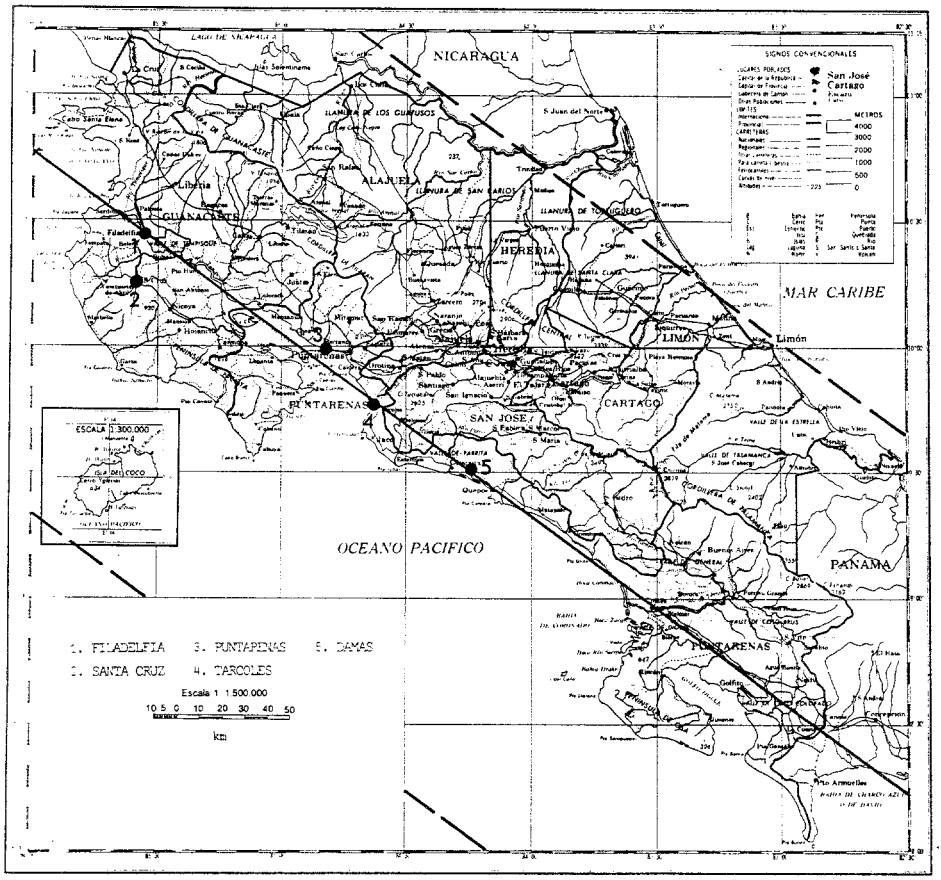

Fig. 1. Map of Costa Rica showing the sites where the measurements of solar irradiance were taken. The two external lines were the borders of the path of totality and the middle line was the central line of totality.

In practice, diffuse irradiance is considered isotropic (Paltridge and Platt, 1971) for two reasons: (a) under a clear sky its vertical component is one order of magnitude smaller than the direct contribution, making anisotropic errors insignificant, (b) under cloudy conditions when all radiation is diffuse, estimations of directional contributions are difficult from ordinary meteorological observations due to the imprecision of cloud description. In any case, multiple diffusion within the clouds induces isotropy and Equation (1) can be written

$$I_g = I_n \cos\theta + I_d\,, \tag{2}$$

where I_d can be estimated or measured. I_g, I_n and I_d depend on solar altitude.

Iqbal (1983, Fig. 6.21.4) estimated the relative magnitudes of I_n and I_d for different wavelengths and considering typical atmospheric conditions. For wave-

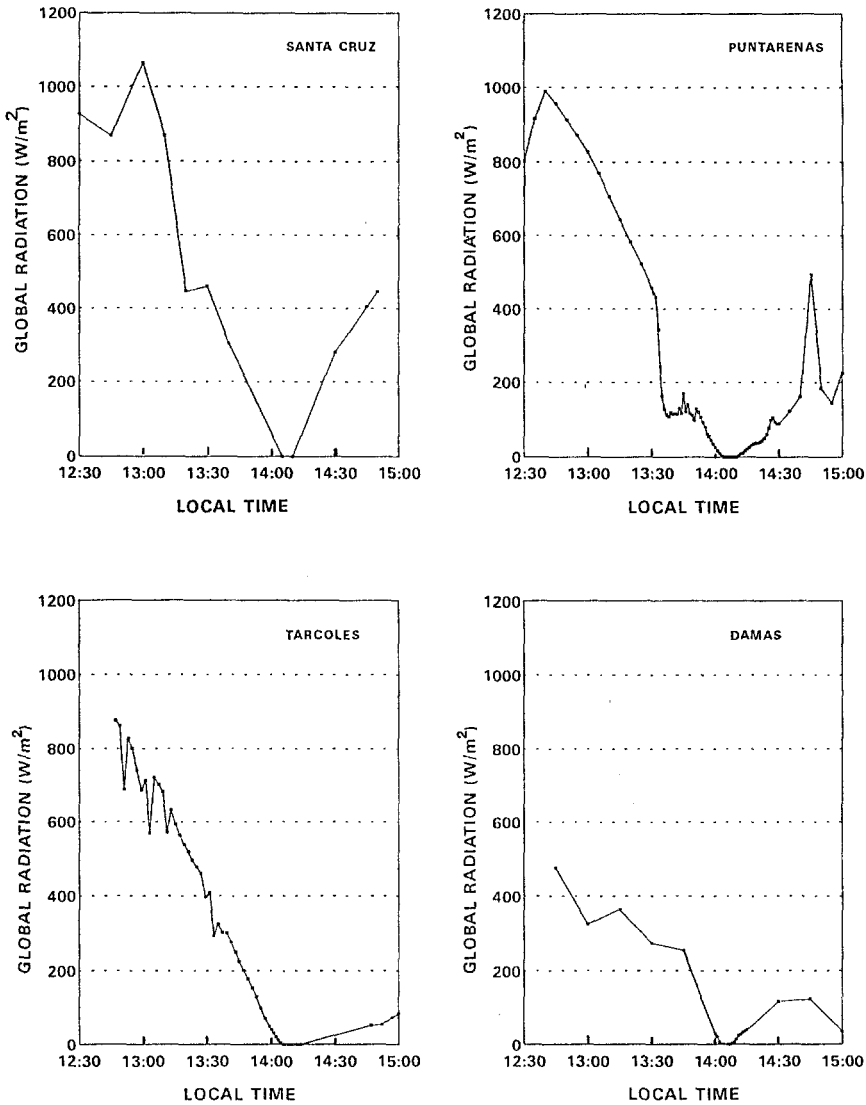

Fig. 2. Temporal variation of global radiation in Santa Cruz, Puntarenas, Tárcoles, and Damas, on July 11, 1991.

lengths below 1000 nm, the ratio I_d/I_g depends on the characteristics of air mass, air turbidity and ground albedo. Other parameters such as ozone and water vapor are irrelevant.

Figure 4 shows the records of the direct and diffuse components in Santa Cruz. Diffuse radiation was estimated from measurements of global and direct radiation. The decrease in radiation intensity during the eclipse is evident.

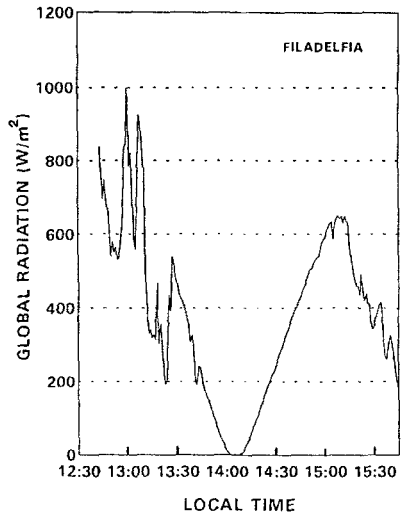

Fig. 3. Temporal variation of global radiation in Filadelfia, on July 11, 1991.

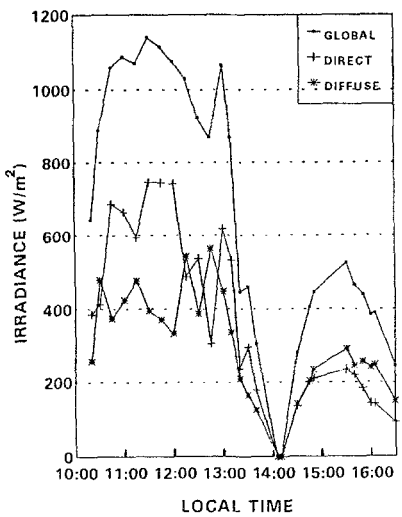

Fig. 4. Temporal variation of global radiation, direct radiation, and diffuse radiation in Santa Cruz, on July 11, 1991.

5. Spectral Irradiance

Visible radiation (390–770 nm) constitutes about 46% of the total electromagnetic energy emitted by the sun, 46% is contained in larger wavelengths and the remain-

TABLE I

Solar irradiance at different wavebands of the solar spectrum outside of the atmosphere, with a solar constant value of 1367 W/m^2 (Iqbal, 1983)

Color	nm	Irradiance W/m^2	Percentage of the solar constant
Violet	390–455	108.55	7.96
Blue	455–492	73.63	5.39
Green	492–577	160.00	11.70
Yellow	577–597	35.97	2.63
Orange	597–622	43.14	3.16
Red	622–770	212.82	15.57
Larger ranges			
Ultraviolet	<400	109.81	8.03
Visible	390–770	634.40	46.41
Infrared	>770	634.40	46.40
Energy from the sun (%)			
95	300–2400		
1.2	<300		
3.6	<2400		

ing 8% is contained in wavelengths below 400 nm. Table I (Iqbal, 1983) shows the approximate partition of the solar spectrum energy in different wavelength intervals. UV irradiance is a small fraction of the global radiation, but it receives special attention because of its biological effects. Therefore, it has been profusely measured (Ilyas and Barton, 1983; Nagaraja Rao and Takashima, 1984, 1985; Castro, 1986; Scott *et al.*, 1988).

UV irradiance was measured in Santa Cruz and Puntarenas during the eclipse (Figures 5 and 6). Figure 5 shows the variations produced by moving broken clouds. It also shows that during totality, and during the minutes before and after, the sun was not shadowed by clouds. Again, irradiance decreases as the eclipse progresses, reaches zero during the totality and increases afterwards.

In Santa Cruz, from the measurements obtained with the filters OG530 and RG630, irradiance in the wavebands 385–530 nm (violet, blue and part of the green), 530–630 nm (part of the green, yellow, orange and part of the red) and 630–2800 nm (part of the red, infrared), were estimated. Results are shown in Figure 7, along with UV irradiance (295–385 nm). All curves follow the pattern of global radiation.

Figure 8 shows irradiance in the above ranges as percentages. Sunlight is composed of different colors that contribute to the total irradiance in different proportions. The contribution of each color is variable: on clear days there is more blue, green and yellow than on overcast days; beneath a forest canopy, light is rich in green and red.

In Santa Cruz, it was observed that during the eclipse, the contribution of each

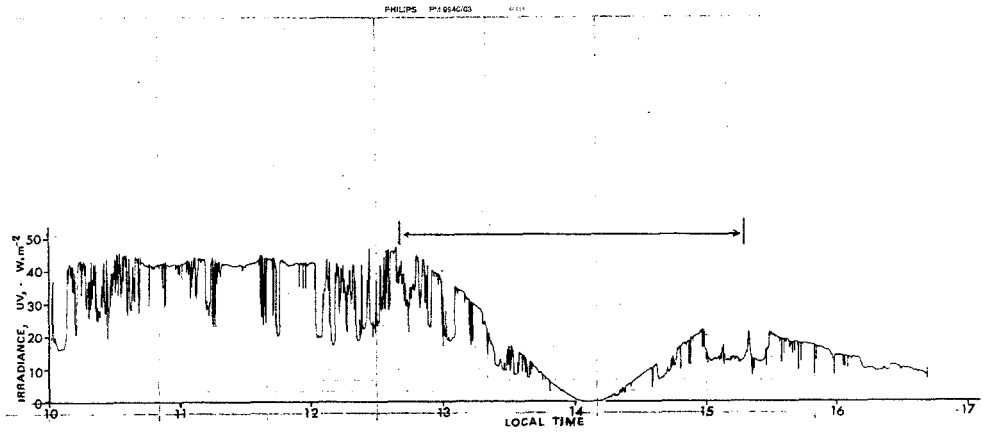

Fig. 5. Recording of ultraviolet irradiance (295–385 nm) in Santa Cruz, on July 11, 1991. The duration of the eclipse is indicated with a horizontal arrow.

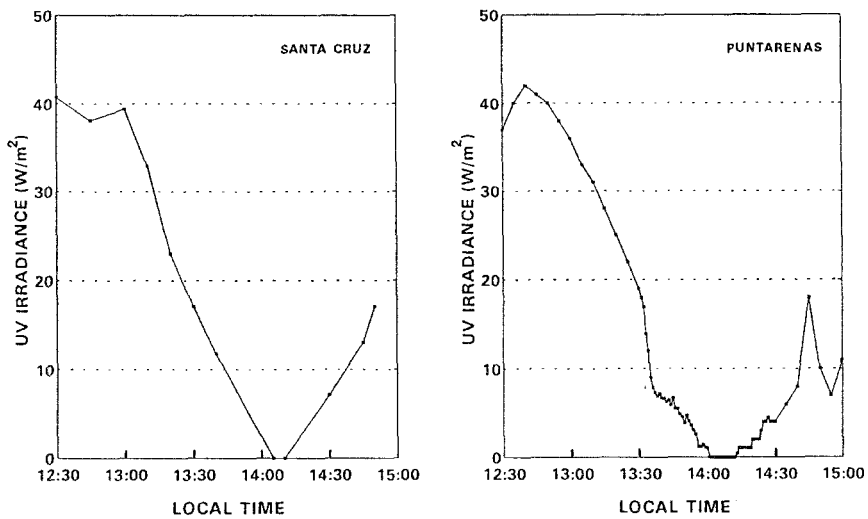

Fig. 6. Temporal variation of ultraviolet irradiance (295–385 nm) in Santa Cruz and Puntarenas, on July 11, 1991.

color was similar to that of a clear day. For that reason, objects during the eclipse did not look as in a normal dusk, when light is rich in reds and oranges. Instead they looked somewhat gray, as irradiance intensity decreased, meaning that there was not a predominant contribution by any color to the total irradiance spectrum.

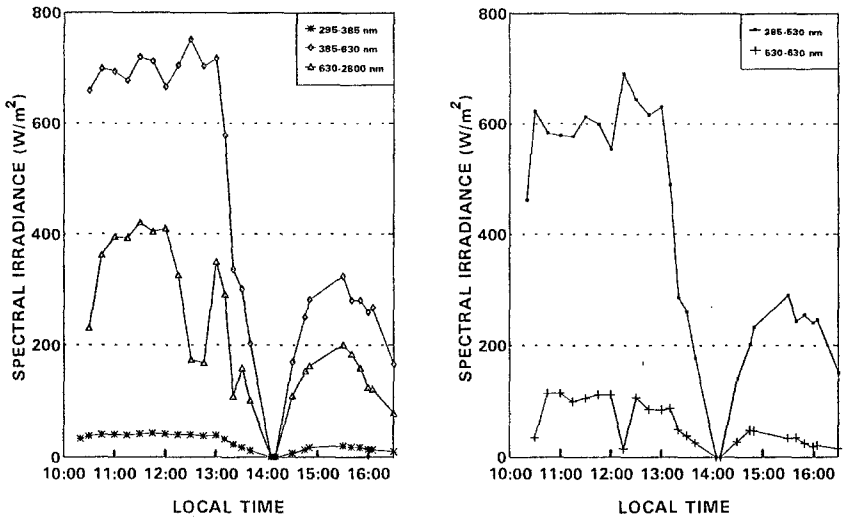

Fig. 7. Temporal variation of solar irradiance at several intervals of wavelength in Santa Cruz, on July 11, 1991. Left side: 295–385 nm (ultraviolet), 385–630 nm (visible), and 630–2800 nm (infrared). Right side: 385–530 nm (violet, blue and part of green), and 530–630nm (part of green, yellow, orange, and part of red).

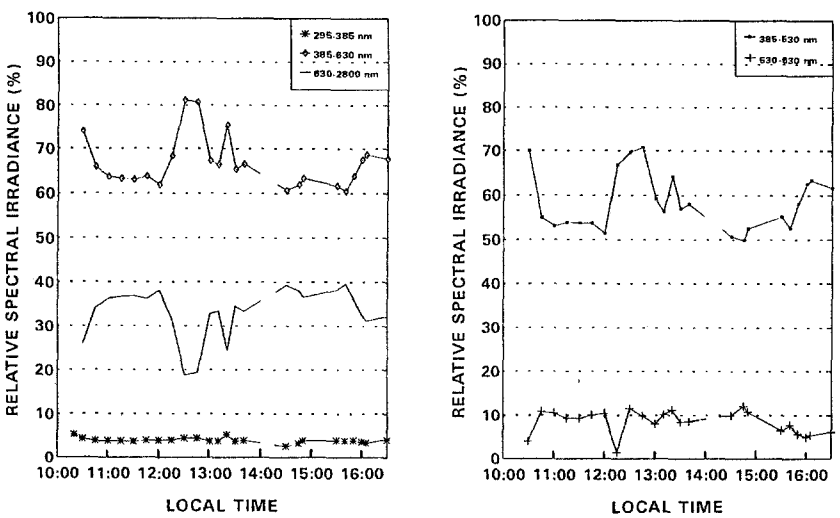

Fig. 8. Temporal variation of solar irradiance at several intervals of wavelength, given as percentages of global radiation, in Santa Cruz on July 11, 1991. Left side: 295–385 nm (ultraviolet), 385–630 nm (visible), and 630–2800 nm (infrared). Right side: 385–530 nm (violet, blue and part of green), and 530–630 nm (part of green, yellow, orange, and part of red).

6. Atmospheric Turbidity Parameters α and β

The quantity of aerosols in the atmosphere and Ångstrom's turbidity parameters α and β can be calculated experimentally from measurements of direct solar radiation and data obtained with filters OG530 and RG630, in a manner similar to that done by Wright in Costa Rica (1990).

(a) Background

Ångstrom's turbidity equation is similar to Beer's attenuation law:

$$\tau_p(\lambda) = \beta\lambda^{-\alpha}, \tag{3}$$

where $\tau_p(\lambda)$ is the optical depth due to atmospheric particles; β, Ångstrom's turbidity coefficient; α, exponent of the wavelength; λ, wavelength (μm).

In the above equation, β represents the vertical quantity of atmospheric aerosols. It can take values from 0 for clear skies, to 0.5 or more for turbid air.

The exponent α expresses the spectral dependance of $\tau_p(\lambda)$, which reflects the size distribution of aerosols in a vertical column. Large values of α correspond to large ratios of small over large particles. It can take values from 4 for very small particles (near the size of air molecules), to 0 for large particles. A value of 1.3 was originally suggested by Ångstrom (1929). Ideriah (1983) says that the range of α for most atmospheres if from 0.5 to 1.3.

The β parameter strongly influences direct spectral irradiance. An increase in β produces a decrease in irradiance (Wright *et al.*, 1989). The exponent α, on the other hand, has a minor effect on spectral irradiance, particularly when $\lambda > 1$ μm.

According to Bouguer–Lambert–Beer law, total optical depth, $\tau(\lambda)$, for a given wavelength is:

$$\tau(\lambda) = -(1/m)\ln\{I_0(\lambda)/[I(\lambda)E_0]\}, \tag{4}$$

where $I_0(\lambda)$ is the direct spectral irradiance at the top of the atmosphere; $I(\lambda)$, direct spectral irradiance at the ground surface; E_0, correction factor for the mean distance earth-sun due to the eccentricity of the earth's orbit; m, relative optical air mass.

E_0 can be obtained from (Spencer, 1971):

$$\begin{aligned} E_0 = (r_0/r)^2 = {} & 1.000110 + 0.034221\cos\Gamma \\ & + 0.001280\sin\Gamma + 0.000719\cos 2\Gamma \\ & + 0.000077\sin 2\Gamma, \end{aligned} \tag{5}$$

where Γ is the day angle in radians

$$\Gamma = 2\pi(d_n - 1)/365 \tag{6}$$

d_n is the Julian day, its value is 1 for January 1, and 365 for December 31.

In addition, m is given by:

$$m = [1 - \sin^2 \theta/(1 + H_1/R_T)^2]^{-1/2}\,, \tag{7}$$

where H_1 is the height of the terrestrial atmosphere (Rayleigh atmosphere height is 7.8 km); R_T, earth's mean radius (6370 km); θ, zenith angle.

Zenith angle can be obtained from:

$$\cos\theta = \sin\delta \sin\Phi + \cos\delta \cos\Phi \cos\Omega_0\,, \tag{8}$$

where δ is the solar declination in degrees; Φ, geographical latitude in degrees; Ω_0, solar angle, zero at noon, positive in the morning.

Total optical depth $\tau(\lambda)$ can be obtained by measuring direct spectral irradiance at the ground surface.

Optical depth for a given wavelength due to atmospheric particles, $\tau_p(\lambda)$, is given by the difference between total optical depth $\tau(\lambda)$ and the optical depth due to the constituents of the atmosphere, in other words:

$$\tau_p(\lambda) = \tau(\lambda) - \tau_R(\lambda) - \tau_{0z}(\lambda) - \tau_w(\lambda) - \tau_n(\lambda)\,, \tag{9}$$

with $\tau_R(\lambda)$ optical depth of a Rayleigh atmosphere, given by:

$$\tau_R(\lambda) = p_0 UR(\lambda)\,, \tag{10}$$

where p_0 is the pressure at the ground surface in bars (1 bar = 10^3 hPa); $UR(\lambda)$, optical depth of Rayleigh standard atmosphere, values may be found in Fröhlich and Shaw (1980).

$\tau_{0z}(\lambda)$ is the optical depth produced by ozone absorption, and can be obtained from:

$$\tau_{0z}(\lambda) = X(\lambda) q\,, \tag{11}$$

where $X(\lambda)$ is the absorption coefficient of oxone; q, vertical content of ozone.

Values of $X(\lambda)$ and q can be obtained from tables given by Vigrous (1953).

$\tau_w(\lambda)$ is the optical depth due to the weak absorption of water vapor. It is given by:

$$\tau_w(\lambda) = c(\lambda) w\,, \tag{12}$$

where $c(\lambda)$ is the absorption coefficient of water vapor; w, precipitable water: vertical content of water vapor (Tomasi, 1979a,b).

$$w = \int_{z_0}^{z} \rho_v(z)\, \mathrm{d}z\,, \tag{13}$$

where $\rho_v(z)$ is the water vapor density (absolute humidity); z_0, altitude of the observation site; z, height of the troposphere.

τ_n is the optical depth due to the absorption of nitrogen dioxide (NO_2). It is given by:

TABLE II

Spectral characteristics of the filters and instruments used

Filter or type of radiation	Opacity interval, nm	Transmissivity interval, nm	Correction factor
OG530	<530	530–2800	0.94
RG630	<630	630–2800	0.925
WG295 (global radiation; Epply pyranometer)	<285	285–2800	–
UV radiation; Eppley pyranometer	<295	295–385	–

$$\tau_n(\lambda) = \sigma(\lambda)n\,, \tag{14}$$

where $\sigma(\lambda)$ is the absorption coefficient of NO_2; n, vertical content of NO_2.

Values of n can be found in Hall and Blacket (1952). For urban areas, Brewer *et al.* (1973) suggest the following values for $\sigma(\lambda)$: 4×10^{-4} cm early in the morning, 3×10^{-3} cm for the middle of the day, and 6×10^{-4} cm for the afternoon.

(b) Estimates in Santa Cruz

Table II shows the spectral characteristics of the filters used with the NIP. The correction factors were recommended by Drummond and Roche (1965). Transparent glass does not require a correction factor.

$I(\lambda)$ values used in the estimation of $\tau(\lambda)$ were obtained when there were no clouds between the sun and the observer, thus cloud attenuation was not considered.

Precipitable water w was estimated from temperature and humidity measurements taken from the ground up to 10 km, with a radiosonde launched at 13:26 LT, 11 July 1991, from Juan Santamaría International Airport, which is located 150 km east of Santa Cruz.

Combining irradiance measurements in the wavebands considered, it is possible to estimate solar spectral intensity $I(\lambda)$ in the following wavebands:

$$\lambda_1 = 285\text{–}530\ \text{nm}\,,$$
$$\lambda_2 = 285\text{–}630\ \text{nm}\,.$$

Total optical depth $\tau(\lambda)$ of the atmosphere for a given wavelength was estimated from Equation (4) for each value of $I(\lambda)$. With these values of total optical depth, the optical depth of aerosol particles $\tau_p(\lambda)$ was calculated with Equation (9).

With the procedure described above, optical depth of the aerosol particles in the wavebands λ_1 and λ_2 were obtained. Turbidity parameters α and β can be found from:

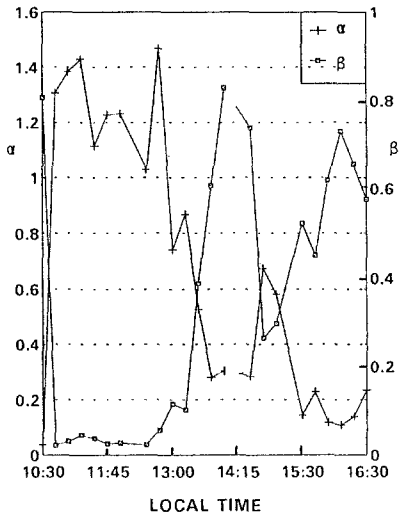

Fig. 9. Temporal variation of Ångstrom's atmospheric turbidity parameters, α and β, in Santa Cruz on July 11, 1991.

$$\beta = \exp\{[\ln \tau_p(\lambda_2) \ln \lambda_1 - \ln \tau_p(\lambda_1) \ln \lambda_2]/\ln(\lambda_1/\lambda_2)\} \tag{15}$$

and

$$\alpha = \ln[\tau_p(\lambda_2)/\tau_p(\lambda_1)]/\ln(\lambda_1/\lambda_2)\,. \tag{16}$$

(c) Results

Figure 9 shows the estimated values of the growth exponent α and turbidity coefficient β for Santa Cruz, Guanacaste, on July 11, 1991.

Between 13:00 and 14:30 LT, β values are relatively high and α values relatively low. This indicates that in the indicated time interval there was a high atmospheric turbidity and that the number of large particles was higher than the number of small particles.

Aerosols may have been salt particles from the sea and dust particles from the ground. The efficiency of such particles as condensation nuclei depends on their properties. Hygroscopic particles are of special interest: when relative humidity is high, they absorb water and grow. Therefore, their size augmented during the eclipse, when temperature decreased sensibly and, consequently, relative humidity increased, in a comparatively short time.

The curves for α and β can be compared with the diurnal variations obtained by Wright (1990) in Heredia, February 1990. In Heredia, α values were higher near noon (1.65), indicating a predominance of small over large particles, and lower early in the morning (0.65 at 8:00 LT) and at late afternoon (0.53 at 17:00 LT), indicating that at those moments large particles predominated over small

ones. On the other hand β values were lower near noon (0.010), indicating low atmospheric turbidity, and higher early in the morning (0.126 at 8:00 LT) and at late afternoon (0.182 at 17:00 LT), indicating high atmospheric turbidity.

The increase of β and decrease of α in Santa Cruz on July 11, 1991, between 13:00 and 14:30 LT is anomalous, as it was produced, as mentioned before, by the temperature decrease and associated relative humidity increase related to the eclipse.

7. Conclusions

The solar eclipse of July 11, 1991, brought the opportunity of studying changes in solar irradiance associated with the eclipse in several locations in Costa Rica.

Even thought the decrease in irradiance during the eclipse was obvious, we were interested in quantifying the evolution of the event. Measurements showed that global radiation, and consequently direct and diffuse radiation as well as radiation in the chosen wavebands, decreased as the eclipse progressed, and increased again to reach normal values.

Estimated values of Ångstrom's atmospheric turbidity parameters, for Santa Cruz, Guanacaste, show that atmospheric turbidity was high, and that large particles were more abundant than small ones between 13:00 and 14:30 LT. This indicates that the size of the hygroscopic particles increased during the eclipse, as a consequence of the temperature decrease and the related relative humidity increase.

Acknowledgments

Several colleagues collaborated with the acquisition of global radiation data. Beatriz Cuendis made measurements at Damas. The data for Filadelfia were obtained, installing an automatic weather station of ICE in the farm El Escarbadero, by Luis E. Acuña, Marco V. Alvarado, Rafael Enrique Chacón and Porfirio Machado (all of ICE) and by Jorge A. Amador (UCR); such data were kindly provided by the Department of Hydrology of ICE. Hugo Hidalgo-León helped with the figures.

References

Ångstrom, A.: 1929, 'On the Atmospheric Transmission by Sun Radiation and in Dust in the Air', *Geografiska* **12**, 130–159.

Brewer, A. W., McEnroy, C. T., and Kerr, J. B.: 1973, 'Nitrogen Dioxide Concentration in the Atmosphere', *Nature* **246**, 129–133.

Castro, V.: 1986, 'Método para la estimación de la radiación ultravioleta a partir de registros de radiación solar global', *Cien. Tec.* **10**, 103–106.

Drummond, A. J. and Roche, J. J.: 1965, 'Corrections to be Applied to Measurements Made with Eppley (and other) Spectral Radiometers when used with Schott Coloured Glasses', *J. Appl. Meteorol.* **4** 741–744.

Fernández, W., Azofeifa, D. E., and Villalobos, J. A.: 1992, 'El eclipse total de Sol del 11 de julio de 1991: Aspectos Generales', en W. Fernández (ed.), *El Eclipse Total de Sol del 11 de Julio de 1991: Observaciones Científicas Realizadas en Costa Rica*, Editorial de la Universidad de Costa Rica, San José.

Fernández, W., Castro, V., and Hidalgo, H.: 1993, 'Air Temperature and Wind Changes in Costa Rica during the Total Solar Eclipse of July 11, 1991, *Earth, Moon, and Planets* **63**, 133–147 (this issue).

Fröhlich, C. and Shaw, G. E.: 1980, 'New Determination of Rayleigh Scattering in the Terrestrial Atmosphere', *Applied Optics* **19**, 1773–1775.

Hall, T. C. and Blacket, F. E.: 1952, 'Separation of the Absorption Spectra of NO_2 and N_2O_4 in the Range of 2400–5000 Ångstroms', *J. Chem. Phys.* **20**, 1745–1749.

Ilyas, M. and Barton, I. J.: 1983, 'Surface Dosage of Erythemal Solar Ultraviolet Radiation near the Equator', *Atmospheric Environment* **17**(10), 2069–2073.

Iqbal, M.: 1983, *An Introduction to Solar Radiation*, Academic Press, New York, 389 pp.

Nagaraja Rao, C. R., Takashima, T., Bradley, W. A., and Young Lee, T.: 1984, 'Near Ultraviolet Radiation at the Earth's Surface: Measurements and Model Comparisons', *Tellus* **36B**, 286–293.

Nagaraja Rao, C. R. and Takashima, T.: 1985, 'Measured and Computed Values of Clear Sky Ultraviolet Irradiances at the South Pole', *Solar Energy* **34**, 435–437.

Paltridge, G. W. and Platt, C. M. R.: 1976, *Radiative Processes in Meteorology and Climatology*, Elsevier Scientific Publishing Company, Amsterdam, 318 pp.

Scotto, J., Cotton, G., Urbach, F., Berger, D., and Fears, T.: 1988, 'Biologically Effective Ultraviolet Radiation: Surface Measurements in the United States, 1974 to 1985', *Science* **239**, 762–763.

Spencer, J. W.: 1971, 'Fourier Series Representation of the Position of the Sun, *Search* **2**(5), 172.

Tomasi, C.: 1979a, 'Non-selective Absorption by Atmospheric water Vapour at Visible and near Infrared Wavelength', *Quart. J. Roy. Meteorol. Soc.* **105**, 1027–1040.

Tomasi, C.: 1979b, 'Weak Absorption by Atmospheric Water Vapour in the Visible and near Infrared Spectral Region', *Il Nuovo Cimento* **C2**, 511–526.

Vigroux, E.: 1953, 'Contribution a l'etude experimentale de l'absorption de l'oxone', *Annales de Physique* **8**, 261–270.

Wright, J.: 1990, 'Experimental Determination of the Atmospheric Turbidity Parameters α and β in Heredia, Costa Rica, with Optical Filters OG530, RG630 and WG350', *The Heliograph* **2**, 16–23.

Wright, J., Perez, R., and Michalsky, J.: 1989, 'Luminous Efficacy of Direct Irradiance: Variations with Insolation and Moisture Conditions', *Solar Energy* **42**, 387–394.